A Study of π Aquarii During a Quasi-normal Star Phase: Refined Fundamental Parameters and Evidence for Binarity

Karen S. Bjorkman and Anatoly S. Miroshnichenko

Ritter Observatory, Dept. of Physics & Astronomy, University of Toledo, Toledo, OH 43606-3390 USA

karen@astro.utoledo.edu, anatoly@physics.utoledo.edu

David McDavid

Limber Observatory, PO Box 63599, Pipe Creek, TX 78063-3599 USA

mcdavid@limber.org

and

Tatiana M. Pogrosheva

Sternberg Astronomical Institute, Universitetskij pr. 13, Moscow 119899, Russia

ABSTRACT

We present the results of recent multicolor photometric and high-resolution spectroscopic observations of the bright Be star π Aquarii. observational data collected from the literature were used to study the star's variations over the last four decades. The star is identified with the IR sources F22227+0107 in the *IRAS* Faint Point Source catalog and *MSX* 5_G066.0066-44.7392 in the MSX catalog. The variations in near-IR brightness of π Aqr are found to be among the largest reported for Be stars. Since 1996, the star has shown only weak signs of circumstellar emission, which has allowed us to refine the fundamental stellar parameters: Av=0.15 mag., T_{eff}=24000 K, log g= 3.9, and M_v=-2.95 mag. A weak emission component of the Ha line has been detected during the recent quasi-normal star phase. From analysis of the Ha line profiles, we find anti-phased radial velocity variations of the emission component and the photospheric absorption, with a period of 84.1 days and semi-amplitudes of 101.4 and 16.7 km s^{-1}, respectively. This result suggests that π Aqr may be a binary system consisting of stars with masses of $M_1 \sin^3 i$ = 12.4 $M_\odot$, $M_2 \sin^3 i$ = 2.0 $M_\odot$. We also estimate the orbital inclination angle to be between 50 and 75°. We suggest that the photometric, spectroscopic, and polarimetric variations observed during the second half of the 20th century may be due to variable mass transfer between the binary components.

Subject headings: stars: individual (π Aqr) —— circumstellar matter — stars: emission- line, Be —— binaries: spectroscopic —— techniques: spectroscopic —— techniques: photometric

1. Introduction

π Aquarii (HR 8539, HD 212571) is a bright rapidly rotating ($v \sin i \sim 300$ km s^{-1}) Be star whose variable characteristics have been noted since the beginning of the 20$^{\rm th}$ century. However, its behavior until the 1960's is only well-documented spectroscopically. McLaughlin (1962) reported variations of the Balmer line profiles (Hβ and Hγ), which appeared double-peaked most of the time, between 1911 and 1961. He reported strong V/R changes ranging from 0.5 to 4.0, and several periods with an absence of bright emission lines (1936–1937, 1944–1945, 1950). This study showed that the star was active, but it did not determine the physical characteristics of the star and its envelope.

Since the late 1950's the star has been frequently observed with various techniques (multicolor photometry, high-resolution spectroscopy, polarimetry) that allow a quantitative study. Several attempts have been made to determine the fundamental parameters of the star. These have resulted, however, in different values being derived, mainly due to the influence of the circumstellar envelope. The following ranges of the parameters were reported in the literature: $T_{\rm eff}$=22500–30000 K, $\log g$= 3.3–4.0, $M_V = -3.00$ – -3.83 mag., and A_V=0.25–0.69 mag. (Nordh and Olofsson 1974; Underhill et al. 1979; Snow 1981; Goraya 1985; Theodossiou 1985; Kaiser 1989; Fabregat and Reglero 1990; Zorec and Briot 1991).

Some of the envelope's parameters are noted in the literature. A wind terminal velocity of 1450 km s^{-1} and a mass loss rate of 2.61×10^{-9} $M_\odot$ yr^{-1}, which is one of the largest among the Be stars, were estimated from UV resonance line profiles (Snow 1981). An envelope temperature of $T_{\rm e} \sim 15,000$ K was derived from optical spectrophotometric and IR photometric observations (Nordh and Olofsson 1974; Gehrz, Hackwell, and Jones 1974). Profiles of the He I lines at 4026 and 4471Å and the Mg II line at 4481Å were used to estimate the inclination angle of the rotation axis to the line of sight (i = 25–30°) and the ratio of the angular velocity to the critical value $\omega/\omega_{\rm crit} = 0.75$ (Gao and Cao 1986; Ruusalepp 1989). However, Ruusalepp (1989) pointed out that such high values of $v \sin i$ and $\omega/\omega_{\rm crit}$ would imply $i \geq 50°$.

Hanuschik et al. (1996) noted that π Aqr might be an interacting binary because of its broad and complex Hα line profile, observed in 1980's. A hypothesis of a binary origin for Be stars was introduced by Křiž and Harmanec (1975). So far $\sim$ 40 Be stars have been found to be binaries (e.g., Pavlovski et al. 1997; Okazaki 1997) using mainly spectroscopic and speckle interferometric techniques. Only a few eclipsing Be binaries, which allow photometric detection, are known. Most known Be binaries have orbital periods between a few days and a few hundred days. Since distances toward Be stars usually exceed 100 pc, the angular separation between the binary companions is relatively small ($\leq$ 10 mas). Therefore, speckle interferometry, with its contemporary threshold of $\sim$50 mas, is able to detect only long-period systems (e.g., Mason et al. 1997). Thus spectroscopy, with its capability of measuring radial velocity (RV) variations of a few km s^{-1}, remains the best tool for searching for Be binaries; however, this requires long-term monitoring. The results of our spectroscopic observations provide a good example of such a program.

Around 1985 the star's brightness, polarization, and emission-line strengths began to decrease. They reached a minimum in 1996 and have stabilized since then. However, line profile variations are still detectable. Only a few Be stars that show strong brightness and emission-line variations have been observed in detail, and these resulted in different interpretations of the phenomenon (Dachs 1982; Hummel 1998). The recent transition of π Aqr from a Be star to a quasi-normal star phase, in connection with our continuous long-term monitoring of the star, gave us a unique opportunity to refine our knowledge of this remarkable object and of the physics of the Be phenomenon.

We collected published information concerning the behavior of π Aqr since the beginning of the last active emission phase, summarized our own data obtained during the decline and minimum phases, and analyzed the complete data set. This allowed us to arrive at important conclusions about the properties of the π Aqr system. In this paper we present our general view of the active emission phase development, report the evidence for binarity of π Aqr, and refine the fundamental parameters of the system's primary. Other results concerning the polarimetric behavior of the system and its disk modeling will be reported elsewhere.

Below we describe our observations (§ 2), discuss the behavior of π Aqr during the last four decades (§ 3 and § 3.2) and the Hα line profile variations (§ 3.3), and suggest an interpretation of the observed phenomena (§ 4).

2. Observations

Our monitoring of π Aqr includes the following observations: 1) UBV photometry (shown in Fig. 1) at a robotic 25 cm reflecting telescope (1987–1999) operated by the Automatic Photoelectric Telescope Service in Arizona (Boyd, Genet, and Hall 1986); 2) Spectroscopy with a resolution $R \sim 26,000$ in the range 5280–6600Å with an échelle spectrograph at the 1 m telescope of the Ritter Observatory of the University of Toledo (1996–2000); and 3) $UBVRIJHK$ photometry with a two-channel photometer-polarimeter (Bergner et al. 1988) at a 1 m telescope of the Tien-Shan Observatory in Kazakhstan (August–December 1998). Spectropolarimetric monitoring (1989–2001, Bjorkman 2000) and broadband $UBVRI$ polarimetry (1985–1998, McDavid 1999) were also carried out. The photometric and polarimetric data will be presented and discussed in detail elsewhere. In this paper we use our spectroscopic data and the brightness level in the minimum state of the object to refine its fundamental parameters.

The Ritter data were reduced with IRAF[1]. Eighty-three spectra with signal-to-noise ratios of 50 and higher were obtained between August 1996 and September 2001. The dates of the observations at Ritter, along with information about the emission component of the Hα line, are presented in Table 1.

[1]IRAF is distributed by the National Optical Astronomy Observatories, which are operated by the Association of Universities for Research in Astronomy, Inc., under contract with the National Science Foundation.

Several observations of the Hα line were obtained in 1990–1991 at Kitt Peak National Observatory (G. Peters, private communication) and at the University of Colorado's Sommers-Bausch Observatory (M. Allen, private communication) in support of the Astro-1 mission, when the star was also observed spectropolarimetrically in the UV region (Bjorkman et al. 1991). These data are included in Fig. 1 and 3. Our study also made use of the IUE spectra of π Aqr obtained between 1985 and 1995, which were retrieved from the IUE final archive (Rodríguez-Pascual et al. 1999).

3. Observed Behavior

3.1. The Last Active Be-Phase

The last active Be-phase of π Aqr, during which line emission was clearly noticeable, probably began in the early 1950's. Weak double-peaked emission in Hα and no emission in Hβ were detected by Burbidge and Burbidge (1950) in mid-1949, while McLaughlin (1962) reported the absence of bright emission in 1950. The early broadband polarimetric data (Coyne and Kruczewski 1969; Serkowski 1970) show that the star already had a large polarization (nearly 1%) by the end of the 1950's, which gradually increased until approximately 1985 (McDavid 1986).

During the period covered by photoelectric photometry data (1957–present), π Aqr displayed mostly smooth and slow changes of its brightness, reaching a maximum brightness phase between the mid-1970's and mid-1980's (see Fig. 1). However, the lack of available data in 1975–1985 makes the detailed shape of the optical brightness maximum uncertain. The near-IR brightness was reported to be roughly constant from 1970 to 1985. Nevertheless, a detailed look at the K-band light curve (Fig. 1b) shows its similarity to the V-band curve. From all the data displayed in Fig. 1, we estimate that π Aqr reached the peak of its active Be star phase in approximately 1980–1985, at which time it had reached a maximum in optical and IR brightness, optical polarization, and emission strength of the Hα line.

The IR excess at this maximum phase was strong and similar to that of other Be stars, i.e., due to free-free and free-bound radiation from the circumstellar gas. Surprisingly, the star was not reported among the Be stars detected by the *IRAS* satellite (e.g., Waters, Coté, and Lamers 1987). Since its galactic latitude is rather high ($b = -45°$), we suspected it might have been recorded in the *IRAS* Faint Source Catalog. Indeed, we found an IR source, F22227+0107, whose position coincided with the optical position of π Aqr. We used the data obtained in the late 1970's to early 1980's to construct the active Be-phase spectral energy distribution (SED) in the range 0.2–60 μm, using the averaged data from *IUE* (1978–1985), optical and IR photometry, and the *IRAS* fluxes (see Fig. 2b). The *IRAS* fluxes obtained in 1983 are in excellent agreement with the IR photometry by Gehrz, Hackwell, and Jones (1974) obtained in 1973.

The spectrum of π Aqr was not extensively monitored from 1960 to 1995. Published results showed that the Hα line displayed significant intensity variations on a time scale of months (Gray

and Marlborough 1974). The profile shape was single-peaked from 1973–1989 (e.g., Slettebak and Reynolds 1978; Andrillat and Fehrenbach 1982). However, in 1989 it changed to a double-peaked profile, and only this shape was detected until 1995 (Hanuschik et al. 1996; Viotti, Rossi, and Muratorio 1998). Characteristic Hα line profiles obtained by different studies during the active Be star phase are displayed in Fig. 3. The Hβ and Hγ line profiles were seen only as double-peaked during the entire Be star phase (Slettebak, Collins, and Truax 1992; Hanuschik, Kozok, and Kaiser 1988). According to McLaughlin (1962), the He I 5876Å line varied similarly to the Balmer lines. Since 1996, when our spectroscopic monitoring observations began, only weak signs of emission have been seen in Hα, while the He I line has always appeared in absorption (see Fig. 4–5). Both the polarization and IR brightness dropped significantly since 1985 (Bjorkman 1994a; McDavid 1999). While the polarization data shown here still contain an interstellar polarization component, analysis of that interstellar component (Bjorkman and Wisniewski 2002) shows that the intrinsic polarization itself is declining throughout this later period. Our data indicate that the star's optical brightness stopped fading in 1995, the line emission reached a minimum in 1996, and the optical polarization stabilized in 1995 (McDavid 1999; Bjorkman 2000). Considering all this information, we conclude that the most recent active Be-phase of π Aqr ended in 1995/6 after lasting for nearly 40 years.

3.2. The Current Quasi-Normal Star Phase

How should we refer to the new phase of π Aqr's behavior since 1995/6? Our simultaneous optical and near-IR photometry, obtained in August 1998, resulted in the detection of the lowest brightness level ever reported in all filters. As seen in Fig. 2a, the SED does not show any notable excess flux with respect to normal stars. The current polarization wavelength dependence is essentially that of a solely interstellar contribution (McDavid 1999; Bjorkman and Wisniewski 2002). However, weak emission is still seen in the Hα line. Thus, we refer to the current phase as the "quasi-normal star" phase.

Only a few spectral lines that are potential indicators of circumstellar envelope activity fall into the wavelength ranges covered by the 9 non-overlapping orders of our échelle spectra. They are Fe II 5317Å, He I 5876Å, Na I $D_{1,2}$, Si II 6347 & 6371Å, Fe II 6383Å, and Hα. There are no signs of the presence of the Fe II and Si II lines within 2% of the underlying continuum. The Na I lines have a full-width at zero intensity (FWZI) of about 110 km s^{-1} and an equivalent width (EW) ratio of 1.3, which is consistent with an interstellar origin. The two remaining lines, He I 5876Å and Hα, display detectable profile variations. These variations are better seen in Hα, since the He I line is weaker (see Fig. 4d).

As we mentioned in § 1, the fundamental parameters of the underlying star as determined by different authors scatter significantly. One of the main reasons for the scatter is that all the studies used data obtained during the active Be phase of the star. The added effect of the circumstellar envelope distorts both the continuum SED and the spectral line profiles, making determination of

the star's characteristics uncertain and model dependent. Thus, it is appropriate to make use of the data obtained during the quasi-normal star phase for re-estimation of the main parameters of the star.

The color-index variations of π Aqr between the Be and quasi-normal star phases are typical for the positive correlation between brightness and emission-line strength noted in many Be stars (e.g., Dachs 1982). At maximum brightness $U-B$ was bluer, while $B-V$ was redder than at minimum (Fig. 1). This effect is due to the circumstellar contribution to the overall brightness of the system (see Harmanec 2000a, for a discussion). The values at minimum brightness (V=4.85 mag., $U-B=-0.90$ mag., $B-V=-0.20$ mag., K=5.45 mag.), the presence of an interstellar polarization component, and the sharp Na I $D_{1,2}$ lines in the star's spectrum indicate that the interstellar extinction toward π Aqr is not zero. The averaged color indices in 1998–1999 give $E(B-V)=0.05\pm0.01$ mag, implying a spectral type of B1 V if we assume a mean interstellar extinction law (Savage and Mathis 1979). The near-IR color indices obtained in August 1998 ($J-H=-0.07$ mag., $H-K=-0.03$ mag.) give essentially the same result. The 1998 brightness in the near IR suggests the absence of additional circumstellar emission in this spectral region. Analysis of the recently released results from the MSX mission (Egan et al. 1999) shows that π Aqr was detected (source $MSX5C$_G066.0066−44.7392) in only one (A band, centered at 8.28 μm) of the 6 photometric bands (total range from 4 to 21 μm), with a flux of 0.385 Jy. This is nearly 10 times lower than the average IR flux (interpolated to the MSX A-band wavelength) during the active Be phase. From this information we can derive the star's fundamental parameters by fitting a theoretical SED to the observed one.

To do this, we used the following: our photometric data in the region 0.36–2.2 μm obtained in August 1998; the IUE fluxes in a number of intervals free of spectral lines from 0.12 to 0.31 μm obtained on 1995 May 25 (high-resolution spectra LWP 30769 and SWP 54752); and the MSX 8.28 μm flux. These data provided a determination of the star's effective temperature ($T_{\rm eff}$) and interstellar reddening (A_V). The Hα and He I 5876Å line profiles obtained in 1996–2000 (see Figs. 4–5) suggest that the circumstellar contribution to the flux in the continuum was extremely small. The SED constructed from our data (Fig. 2a) was fitted to Kurucz (1994) model atmospheres with $T_{\rm eff}$ and A_V as free parameters (note that this procedure is not sensitive to the stellar gravity). The best fit values are $T_{\rm eff}=24000\pm1000$ K and $A_V=0.15\pm0.03$ mag. Adopting a distance of 340^{+105}_{-70} pc, obtained by HIPPARCOS (ESA 1997), we derive the following fundamental parameters of the star: $\log(L_{\rm bol}/L_\odot)=4.1\pm0.3$ and $R_*=6.1\pm2.5$ $R_\odot$.

The $T_{\rm eff}$ is unlikely to be less than 23,000 K, because otherwise the corresponding interstellar reddening would be too small for the observed strength of the Na I lines and current polarization level ($P_V\sim0.45\%$). It is seen in Fig. 2c that the IUE data, obtained in 1995 when π Aqr already had very weak emission lines, lie just below the Kurucz model for $T_{\rm eff}=24,000$ K. During the active Be phase, the UV flux level was lower than in 1995 because of the metallic line blanketing effect and a lesser additional circumstellar emission than that in the optical and near-IR range. A noticeable dip due to absorption by Fe II lines in the circumstellar disk is seen in Fig. 2d. Thus

even if some amount of line blanketing was still present in the 1995 *IUE* spectrum, it is unlikely that the level of the stellar flux in this region is larger than the theoretical one for $T_{\rm eff} = 25,000$ K.

Comparison with theoretical evolutionary tracks (Shaerer et al. 1993) provides an estimate of the star's mass, $M_* = 11 \pm 1.5\ M_\odot$ (Fig. 6), and hence the critical rotational velocity, $v_{\rm crit} = 585^{+185}_{-95}$ km s^{-1}, and $\log g = 3.9 \pm 0.1$. Comparison of the observed SED with that of the Collins and Sonneborn (1977) model for a B1-type star ($T_{\rm eff} = 25,000$ K) rotating at half the critical rotation speed (which corresponds to $v \sim 260$ km s^{-1} for the parameters adopted by Collins and Sonneborn (1977) and is close to the $v \sin i$ of π Aqr) shows excellent agreement at all considered wavelengths.

An independent way to estimate the stellar parameters is to fit the observed line profiles to theoretical ones. For this purpose we can use the averaged He I 5876Å line profile and the Hα line wings, which are unaffected by the traveling emission component which is discussed below. The detected regular variations of the Hα absorption component were taken into account. Note that the Hα in our case is mainly indicative of the star's rotational velocity. We calculated a grid of theoretical spectra containing these lines using the radiation transfer code SYNSPEC (Hubeny, Lanz, and Jeffery 1995) for $\log\ g = 4.0$ and $T_{\rm eff}$ from 20,000 to 30,000 K, and broadened them by rotation. The best fits for the Hα line were achieved for $T_{\rm eff} = 25,000 \pm 2,000$ K and $v \sin i = 250 \pm 10$ km s^{-1}. The observed He I line profile turned out to be too deep even for $T_{\rm eff} = 20,000$ K and $v \sin i = 300$ km s^{-1} (Fig. 4d). Such a discrepancy between the theoretical and observed profiles of some He I lines, including the one at 5876Å, has previously been noted by Smith, Hubeny, and Lanz (1994). This might also imply that the line, which is formed very close to the stellar surface where the circumstellar envelope is most dense, is still affected by the circumstellar contribution. Also, the average observed profile is rather noisy because of its weakness and both regular and possible irregular variations.

As mentioned in § 1, the inclination of π Aqr's rotation axis once was estimated to be 25–30° based on an analysis of several He and Mg absorption lines. Ruusalepp (1989) noted that the $v \sin i$ of the star and this purported inclination angle were not consistent with each other. The large variations of the Hα line profile, the double-peaked shape of the Hβ and Hγ lines, and a high polarization during the brightness maximum all suggest a configuration much closer to edge-on. Hanuschik et al. (1996) detected a double-peaked emission profile of the Fe II 5317Å line, which suggests an intermediate inclination angle. Furthermore, the central depressions in the Balmer line profiles observed in 1989–1995 (see Fig. 3) are not very strong, indicating that the disk is not seen exactly edge-on. Calculations by Stee and Araujo (1994), performed with stellar and envelope parameters close to those we find for π Aqr, suggest that the Hα profiles which were observed in 1989–1995 can be reproduced with inclination angles of about 50–60°. Calculations by Hummel (2000) show that the central depression drops below the continuum in Hα profiles for $i \geq 80°$. Based on this information, we suggest that $50° \leq\ i \leq 75°$ for π Aqr.

3.3. Hα Variations During the Quasi-Normal Star Phase

During the quasi-normal star phase, the Hα line is seen in absorption most of the time. The photospheric profile is altered by variable emission, in which we can identify three distinct components. Two of them are very weak most of the time ($\sim 0.02\ I_{\rm cont}$ above the theoretical photospheric profile) and are located at about $\pm$350 km s^{-1} (see Fig. 4c). On only three occasions, 1996 August 30 and 1998 September 9 and 29, these components were observed to be significantly stronger (see Fig. 4a). The former two profiles are almost identical, while the third one has weaker emission peaks. Another feature of these profiles is that they show stronger emission at almost all velocities than is seen in the other spectra. These two emission components are reminiscent of the double-peaked profile that the star displayed during the decline phase in 1989–1995. However, the peak separation in 1996–2000 is noticeably larger than it was previously.

The rest of the Hα profiles obtained show an additional emission component of almost the same width ($\sim$ 200 km s^{-1}) traveling inside the photospheric absorption within $\pm$101 km s^{-1} (see Table 1). To locate this component, we normalized each spectrum to the underlying continuum, removed the profile regions contaminated with telluric water vapor lines, and subtracted a theoretical photospheric profile calculated for the star's fundamental parameters as derived above. The residual profiles obtained in September–November 1999 are shown in Fig. 5. The average parameters of the traveling emission component are as follows: $v_{\rm FWZI} \sim 400$ km s^{-1}, $v_{\rm FWHM} \sim 200$ km s^{-1}, $I \sim 0.08\ I_{\rm cont}$. It is difficult to constrain the shape of the component's line wings because of blending with the double-peaked structure; however, the core is rather symmetric.

In addition to the RV variations of the traveling emission component, the entire Hα absorption profile changes its RV. Since the former occupies an insignificant portion of the latter, we were able to measure their RVs independently. A technique of matching symmetric parts of the original and mirrored profiles was used for both components. When measuring RVs of the absorption wings, the region of the traveling emission component was excluded. Similarly, the photospheric profile was subtracted to measure RVs of the traveling emission component. As a result, we found that both variations are periodic, have the same period (within the uncertainties listed in Table 2), and are anti-phased. The measured RVs of the emission and absorption component are plotted against each other in Fig. 7b. The relationship between them is well determined (a correlation coefficient of 0.9), despite some scatter due to the measurement errors ($\sim$2–3 km s^{-1} for most of the datapoints, up to $\sim$5 km s^{-1} for those with the lowest signal-to-noise ratios).

The periodic RV variations of the traveling emission component have been observed during more than 20 cycles. This indicates that the source of the Hα emission rotates around the star in a stable orbit. The radius of this orbit can be calculated using the derived period and the semi-amplitude of the RV curve: $r_{\rm orb} = 169 {\rm R}_\odot \sin^{-1} i$, where i is the inclination angle of the orbit. Alternatively, if we assume that the Hα emission source rotates in the star's disk, we can derive its orbital radius using Kepler's law, $v(R) = v_{\rm crit}\,(r/R_*)^{-0.5}$. The result, 133 $R_\odot \sin^2 i$, is not consistent with the above $r_{\rm orb}$ at any inclination angle. This indicates that the source is located outside π

Aqr's disk. It seems unlikely that the Hα emission source is just a cloud of gas orbiting about the star. A more plausible explanation of this phenomenon is that there is a secondary companion, surrounded by a gaseous envelope, in a stable orbit about the primary. Moreover, the RV amplitude of the absorption component, which we suppose to be mostly photospheric, is much smaller than that of the emission component. Such behavior is expected for spectroscopic binaries, a number of which are Be stars (e.g., Pavlovski et al. 1997).

If we assume this is evidence that π Aqr is a spectroscopic binary, we can derive appropriate binary parameters for the system. First we checked for eccentricity effects by fitting the RV curves to the general equation of orbital motion. The RV curves for both the absorption and emission components were found to be virtually symmetric within the measurement errors, which indicates that the orbital eccentricity is very small or absent. Thus, the orbit is approximately circular.

The best fit parameter values are shown in Table 2. The RV phase curves for both components are presented in Fig. 7a. These results strongly argue in favor of a binary origin of the system, in which the absorption-line spectrum is associated with a more massive B-type primary, while the traveling emission component in the Hα line originates in a region around a less massive secondary. The differences between the parameters derived from the RVs of the Hα emission and absorption components are most likely due to individual measurement errors, quoted above. We should also note that the RVs of the emission component depend on the adopted theoretical photospheric profile. The latter affects the resulting RV, especially at the extremal positions of the emission component, because of the photospheric profile curvature. However, this effect only results in an uncertainty of ≤ 0.05 days in the orbital period and of $\leq$5 km s^{-1} in the RV semi-amplitude. The emission phenomenon, which gave rise to the three double-peaked profiles mentioned above, does not have any effect on the periodicity. It does not even hide the traveling emission component. The only profile in which the traveling component was not seen is that of 1998 September 29. The component's RV at that time should have been about zero, and we were unable to measure it because of the contamination with additional emission.

Using these orbital parameters, we can estimate the orbiting masses using corresponding equations for Keplerian motion with zero eccentricity. Applying the data from Table 2, one can calculate the mass function $f(M) = 0.041\,M_\odot$ and, using the RV semi-amplitudes, $M_1\,sin^3\,i = 12.4\ M_\odot$, $M_2\,sin^3\,i = 2.0 M_\odot$, and $M_2/M_1 = 0.16$.

The equivalent width of the traveling emission component listed in Table 2 also shows variations with the 84 day period. Additionally, the component strength seems to decrease with time. The phase curve corrected for the temporal trend shows that the emission becomes weaker at phases 0.6–0.7 (Fig. 7c). This phase interval is centered at the moment when the RV=0, and the secondary should be in front of the primary. This phenomenon might be caused by a non-spherical distribution of circumstellar gas around the secondary, so that the star occults more matter at the mentioned phases. In other words, there is additional circumstellar matter between the stars. At the same time, the absence of such an effect around phase 0.25 suggests that there is no obscuration of the

emitting material by the visible star and its disk remnant.

Thus, our spectra obtained during the current quasi-normal star phase of π Aqr have revealed a cyclic emission activity in the Hα line. Other indicators of the circumstellar envelope, except for the very weak double-peaked emission in the Hα line, have vanished. RV variations of the photospheric Hα profile, indicating an orbital motion of the primary component, have also been detected. Similar variations are seen in the He I 5876Å line. However, it is more difficult to measure them since the line is shallower than Hα.

4. Discussion

The RV variations of the Hα profile components gave another estimate of the visible star mass ($M_1 \sin^3 i = 12.4\ M_\odot$). This estimate is probably only accurate to within 20% because of the measurement errors and uncertainties mentioned above. If we assume that the orbital inclination angle is the same as the disk inclination angle ($\sim 70°$, see § 3.2), then $M_1 \sim 15 \pm 3\ M_\odot$. This is somewhat higher than our evolutionary track estimate, but still within the calculation uncertainties. A more accurate spectroscopic estimate might be derived given more observations at a higher signal-to-noise ratio and from a drier site, if the system remains in the quasi-normal star phase.

The derived $T_{\rm eff}$ is in good agreement with the spectral type (B1) assigned to the star in earlier studies (e.g., Guetter 1968). We found that π Aqr is basically less luminous than previously thought, since the star was usually estimated to be brighter because of the effect of the circumstellar envelope. This effect also caused overestimation of the interstellar reddening in most previous papers (see § 1).

The measured semi-amplitude ratio of the absorption and emission component RVs during the quasi-normal star phase suggests that the stellar companion, if placed at the center of the Hα emission source, should be ∼6 times less massive than the visible star. According to the derived RV curve parameters and the estimated orbital inclination angle, the mass associated with the emission component is between 2 and 3 $M_\odot$. Thus, it is most likely a star surrounded by a gaseous envelope. Evolutionary arguments would suggest that this secondary component should be a main-sequence star. The evolutionary tracks (Shaerer et al. 1993) for such a star indicate that it would be an A-type (or even F-type) star with a luminosity more than 2 orders of magnitude smaller than that of the primary. This would imply a visual magnitude difference of at least 4 magnitudes. Therefore, the contribution from such a secondary to the continuum radiation of the system is negligible, and it is not surprising that no signs of it have been detected.

From the estimated brightness ratio of the companions, one can model the Hα profiles observed during the quasi-normal star phase in order to estimate an average density of the circumstellar gas around the secondary. For this purpose, we assume that the emission line due to this gas is described by a Gaussian profile, and that the secondary's photospheric Hα profile is described by a Kurucz (1994) model atmosphere with $T_{\rm eff} = 9,000$ K and $\log g = 4.0$. The secondary's rotation rate and

fundamental parameters are not crucial because of the large brightness ratio. The results for one observed spectrum are shown in Fig. 8. The Hα emission in the secondary spectrum should be rather strong (equivalent width of about 20 Å), which would require a mean number density on the order of 10^{11} cm^{-3}, assuming a spherical density distribution. Such an emission line strength and envelope density is similar to that of Herbig Ae/Be stars, which have mass loss rates of about $10^{-8} M_{\odot}$ yr^{-1} (Böhm and Catala 1995). However, this does not mean that the secondary is at the pre-main-sequence evolutionary stage. Its envelope is most likely formed due to mass exchange in the system.

The semi-major axis of the binary orbit can be derived from the data of Table 2, which gives $a = 0.96 \sin^{-1} i$ A.U. This value corresponds to an angular separation of $\sim$3 mas at the HIPPARCOS distance of π Aqr. This is far below the Rayleigh limit of 55 mas reported for the star by Mason et al. (1997), who searched for binary components around Be stars using speckle interferometry.

The observational data for π Aqr, collected and summarized in Fig. 1, show that variations of its brightness, color-indices, emission-line strength, and polarization correlate with each other. Three major distinct phases can be recognized in the stellar behavior during the last four decades: 1) the active Be star phase, showing an increase of brightness, emission-line strength, and polarization (early 1950's through $\sim$1985); 2) the transition phase, with a rapid decrease of these same characteristics ($\sim$1985 through 1995); and 3) the quasi-normal star phase, with only very weak signs of circumstellar activity (since 1996).

The temporal correlation indicates that all the detected variations can be explained by the same mechanism. This mechanism is most likely the added flux due to a circumstellar gaseous envelope with a variable density, as previously suggested for π Aqr by Nordh and Olofsson (1977). Gradual strengthening of the circumstellar emission until the mid-1980's suggests that the amount of matter in the disk was increasing during this time. Therefore, an SED constructed from data obtained at a particular time during this phase reflects only the amount of matter accumulated in the disk up to that time. An SED constructed from only observations at an earlier or later time would lead to a different mass estimate for the disk.

The Stokes QU parameters measured at different times are distributed along a well-established line (see Bjorkman 2000), implying that the intrinsic polarization position angle (PA) was nearly constant. According to current models (e.g., Wood, Bjorkman, and Bjorkman 1997), the intrinsic polarization of Be stars originates in the circumstellar disk, and the resulting PA is perpendicular to the disk equatorial plane. This has been verified observationally by Quirrenbach et al. (1997). Thus, the observed intrinsic PA constancy leads to the conclusion that the orientation of the disk around π Aqr with respect to the line of sight did not change during the period considered here.

The unusual Hα line profile shape observed in 1973–1989 (see Fig. 3) might imply that mass transfer from the primary's disk into the secondary's Roche lobe through the inner Lagrangian point L_1 occurred during a part of the active Be phase (see Fig. 6 from Harmanec 1985). This suggestion can be supported by the following arguments:

1) The RVs of the Hα profile dominating peak were confined within $\pm$100 km s^{-1} (see Fig. 3), which is well inside the peak separation of the double-peaked structure observed in 1989–1995. This suggests that the dominating peak was formed in a low-velocity region of the disk. If Be star disks are Keplerian (see Hummel and Hanuschik 1997), this region should be close to the disk's outer parts.

2) The size of the primary's Roche lobe, $\sim 0.6\,a$ for the derived components' mass ratio (Pringle and Wade 1985), is $\sim 25\ R_1$. This value is similar to the disk size of γ Cas derived from interferometry (Berio et al. 1999). Since the emission-line spectrum of π Aqr during the active Be phase was even stronger than that of γ Cas, the primary's disk in the π Aqr system might fill the primary's Roche lobe.

3) The absence of mass transfer out of the disk would result in a very different picture of the object's variability since 1989. In this case, in order to get rid of the bulk of the disk matter, one needs to accrete it onto the primary. In the beginning, this process would re-shape the line profiles, making them double-peaked with a larger intensity, as the amount of matter in the disk is still constant. However, we observed a decrease of emission peak intensity only a few months after the Hα profile re-shaping occurred.

We should note here that reasons for the mass loss variations from the primary star are not known. Concerning the disk dissipation process, if we assume a constant velocity of 1 km s^{-1}, a particle would cross the π Aqr disk in 2 years. This is consistent with the observed timescale of the disk dissipation ($\sim$5 yr).

A detection of π Aqr by the *ROSAT* survey in 1990 (during the early decline phase) with $\log(L_{\rm x}/L_{\rm bol}) \sim -6.6$ (corrected using our new value of $L_{\rm bol}$) shows that its x-ray luminosity is only marginally higher than the average value for stars hotter than B1-type (Berghöffer, Schmitt, and Cassinelli 1996). However, the detected x-ray luminosity is only 0.3 dex smaller than that of γ Cas, which has been suspected of having a compact companion (Mason, White, and Sanford 1976), and it may also be variable. π Aqr was one of only a few Be stars detected by EUVE (Christian et al. 1999), which might imply the presence of flux in excess of the photospheric contribution in this wavelength region. Such an excess might be attributed to chromospheric activity of the secondary.

A number of other bright Be stars show variations of the Hα line profile, similar to those of π Aqr, during their active Be phase (e.g. γ Cas, 59 Cyg, ζ Tau). The binary hypothesis may well be applied to these objects. ζ Tau is already known as a spectroscopic binary with a period of 132.91 days (e.g., Underhill 1952), close to the period we found for π Aqr. Recently Harmanec et al. (2000b) found a period of 203.59 days in the emission line variations of γ Cas and attributed them to binary orbital motion.

Now we can make some suggestions in response to the questions raised by McDavid (1999) about the physical reasons for the polarization decline in π Aqr. The multiwavelength behavior of π Aqr during the quasi-normal star phase indicates that the primary's disk indeed lost its replenishment source. The temporal variations of the system indicate that the disk is not a static

structure, but rather has a variable mass and density distribution. The underlying star does not seem to change its fundamental characteristics. However, a triggering mechanism which could turn off the mass loss is not clear yet. At present we have no information which would allow us to discuss this subject in any detail.

5. CONCLUSIONS

We have presented and analyzed photometric, polarimetric, and spectroscopic data for the bright Be star π Aqr obtained during the last four decades. The star showed a brightening between the late 1950's and early 1970's, a maximum phase through 1985, a decline between 1985 and 1995, and a low-brightness phase by the present time. This large data set allowed us to derive new, more reliable physical parameters of the star. We also have identified π Aqr with IR sources in the *IRAS* Faint Source Catalog and in the *MSX* satellite point source catalog.

Regular RV variations of a traveling emission component within the Hα line profile and of the underlying photospheric absorption profile with a period of 84.1 days have been detected during the quasi-normal star phase of π Aqr in 1996–2000. The combined picture of the profile structure and variations suggests that π Aqr may be a close binary system with variable mass exchange.

The following estimates of the fundamental parameters of the system's visual component and the interstellar reddening were made: $M_1 = 11 \pm 1.5\ M_\odot, R_1 = 6.1 \pm 2.5\ R_\odot, T_{\rm eff} = 25,000 \pm 2,000\ K, \log(L_{\rm bol}/L_\odot) = 4.1 \pm 0.3, A_V = 0.15$ mag. Also, some constraints were placed on the system inclination angle, binary mass ratio and separation: $50^\circ \leq\ i \leq 75^\circ, M_2/M_1 = 0.16, a = 0.96\ \sin^{-1} i$ A.U. The secondary is most likely an A–F main-sequence star.

There are some major consequences of our interpretation of the active Be phase. First, the mass loss rate cannot be determined accurately from the SED (IR excess) obtained at a particular time, because the star's gradual brightening indicates a disk mass growth with time. Second, variations of the Hα line profiles of other Be stars, which show a structure similar to that of π Aqr during its active Be phase, should be searched for periodicities. We would like to emphasize here that we do not claim that this mechanism is operating for all Be stars; however, a certain fraction of them may well be explained by a similar hypothesis.

Further observations of π Aqr are of interest in order to follow the quasi-normal star phase and detect any new possible brightening. They would help to reconstruct the the disk replenishment process and improve the parameters of the π Aqr binary system, which was first suspected by Hanuschik et al. (1996) but not detected with speckle interferometry (Mason et al. 1997).

We thank an anonymous referee for comments which helped improve the manuscript. We are grateful to R. W. Hanuschik for providing us with his Hα line profiles of π Aqr obtained in 1982–1995, to A. V. Mironov for sending us unpublished photometric *WBVR* data obtained in 1986,

and to G. Peters and M. Allen for providing the KPNO and SBO Hα spectroscopic observations. We thank the present and past members of the Ritter observing team, especially N. Morrison, C. Mulliss, K. Gordon, D. Knauth, and W. Fischer, for assistance in the data acquisition. We thank J. Bjorkman for useful conversations about these results. AM and KSB acknowledge support from NASA grant NAG5-8054. Karen Bjorkman is a Cottrell Scholar of the Research Corporation, and gratefully acknowledges their support. Support for observational research at Ritter Observatory has been provided by The University of Toledo, by NSF grant AST-9024802 to B. W. Bopp, and by a grant from the Fund for Astrophysical Research. Technical support at Ritter is provided by R. J. Burmeister. This research has made use of NASA's Astrophysics Data System and of the SIMBAD database, operated at CDS, Strasbourg, France.

REFERENCES

Andrillat, Y., and Fehrenbach, C. 1982, A&AS, 48, 93

Berghöffer, T.W., Schmitt, J.H.M.M., & Cassinelli, J.P. 1996, A&AS, 118, 481

Bergner, Yu.K., et al. 1988, Izvestia Glavn. Astron. Observ. at Pulkovo, 205, 142

Berio, P., et al. 1999, A&A, 345, 203

Bjorkman, K.S., et al. 1991, ApJ, 383, L67

Bjorkman, K.S. 1994a, in Pulsation, Rotation and Mass Loss in Early-Type Stars, Proc. IAU Symp. 162, L.A.Balona, H.F.Henrichs, J.M.Le Contel (eds.), (Dordrecht: Kluwer), p. 219

Bjorkman, K.S. 2000, in The Be Phenomenon in Early-Type Stars, Proc. IAU Coll. 175, M.A.Smith, H.F.Henrichs, J.Fabregat (eds.), ASP Conf. Prof. 214, p. 384

Bjorkman, K.S., and Wisniewski, J.P. 2002, in preparation

Böhm, T., and Catala, C. 1995, A&A, 301, 155

Boyd, L.J., Genet, R.M., and Hall, D.S. 1986, PASP, 98, 618

Burbidge, E.M., and Burbidge, G.R. 1950, ApJ, 113, 84

Christian, D.J., Craig, N., Cahill, W., Roberts, B., and Malina, R.F. 1999, AJ, 117, 2466

Collins, G.W., and Sonneborn, G.H. 1977, ApJS, 34, 41

Coyne, G.V., and Kruczewski, A., 1969, AJ, 74, 528

Dachs, J. 1982, in Be stars, Proc. IAU Symp. 98, M.Jaschek and H.-G.Groth (eds.), p.19

Egan, M.P., et al. 1999, The Midcourse Space Experiment Point Source Catalog Version 1.2, Explanatory Guide, AFRL-VS-TR-1999-1522

ESA, 1997, The Hipparcos and Tycho Catalogues, ESA SP-1200

Fabregat, J., and Reglero, V. 1990, MNRAS, 247, 407

Gao, W.-S., and Cao, H.-L. 1986, Acta Astron. Sinica, 6, 143

Gehrz, R.D., Hackwell, J.A., and Jones, T.W. 1974, ApJ, 191, 675

Goraya, P.S. 1985, MNRAS, 215, 265

Gray, D.F., and Marlborough, J.M. 1974, ApJS, 27, 121

Guetter, H.H. 1968, PASP, 80, 197

Hanuschik, R.W., Kozok, J.R., and Kaiser, D. 1988, A&A, 189, 147

Hanuschik, R.W., et al. 1996, A&AS, 116, 309

Harmanec, P. 1985, Bull. Astron. Inst. Czech., 36, 327

Harmanec, P. 1998, A&A, 335, 173

Harmanec, P. 2000a, in The Be Phenomenon in Early-Type Stars, Proc. IAU Coll. 175, M.A.Smith, H.F.Henrichs, J.Fabregat (eds.), ASP Conf. Prof. 214, p. 13

Harmanec, P., et al. 2000b, A&A, 364, L85

Hubeny, I., Lanz, T., and Jeffery, C.S., 1995, Synspec – A User's Guide

Hummel, W., and Hanuschik, R.W., 1997, A&A, 320, 852

Hummel, W. 1998, A&A, 330, 243

Hummel, W. 2000, in in The Be Phenomenon in Early-Type Stars, Proc. IAU Coll. 175, M.A.Smith, H.F.Henrichs, and J.Fabregat (eds.), ASP Conf. Ser. 214, 396

Kaiser, D. 1989, A&A, 222, 187

Křiž, S. and Harmanec, P. 1976, Bull. Astron. Inst. Czech., 26, 65

Kurucz, R.L. 1994, Smithsonian. Astrophys. Obs., CD-ROM No.19

Mason, B.D., et al. 1997, AJ, 114, 2112

Mason, K.O., White, N.E., and Sanford, P.W. 1976, Nature, 260, 690

McDavid, D. 1986, PASP, 98, 572

McDavid, D. 1999, PASP, 111, 494

McLaughlin, D.B. 1962, ApJS, 7, 65

Nordh, H.L., and Olofsson, S.G. 1974, A&A, 31, 343

Nordh, H.L., and Olofsson, S.G. 1977, A&A, 56, 117

Okazaki, A.T. 1997, A&A, 318, 548

Pavlovski, K., et al. 1997, A&AS, 125, 75

Pringle, J.E., and Wade, R.A. 1985, Interacting binary stars, Cambridge University Press

Quirrenbach, A., et al. 1997, ApJ, 479, 477

Rodríguez-Pascual, P.M., González-Riestra, R., Schartel, N., and Wamsteker, W. 1999, A&AS, 139, 183

Ruusalepp, M. 1989, Tartu Astrophys. Observ. Publ., 100, 1

Savage, B.D., and Mathis, J.S. 1979, ARA&A, 17, 73

Serkowski, K. 1970, ApJ, 160, 1083

Shaerer, D., et al. 1993, A&AS, 102, 339

Slettebak, A., and Reynolds, R.C. 1978, ApJS, 38, 205

Slettebak, A., Collins, G.W., and Truax, R. 1992, ApJS, 81, 335

Smith, M.A., Hubeny, I., and Lanz, T. 1994, In Pulsation, Rotation and Mass Loss in Early-Type Stars, Proc. IAU Symp. 162, L.A.Balona, H.F.Henrichs, and J.M.Le Contel (eds.), p. 273

Snow, T.P. 1981, ApJ, 251, 139

Stee, Ph., and Araujo, F.X. 1994, A&A, 292, 221

Theodossiou, E. 1985, MNRAS, 214, 327

Underhill, A.B. 1952, Publ. Dominion Astrophys. Obs. 9, 219

Underhill, A.B., et al. 1979, MNRAS, 189, 601

Viotti, R., Rossi, C., and Muratorio G. 1998, A&AS, 128, 447

Waters, L.B.F.M., Coté, J., and Lamers, H.J.G.L.M., 1987, A&A, 185, 206

Wood, K., Bjorkman, K.S., and Bjorkman, J.E. 1997, ApJ, 477, 926

Zorec, J., and Briot, D. 1991, A&A, 245, 150

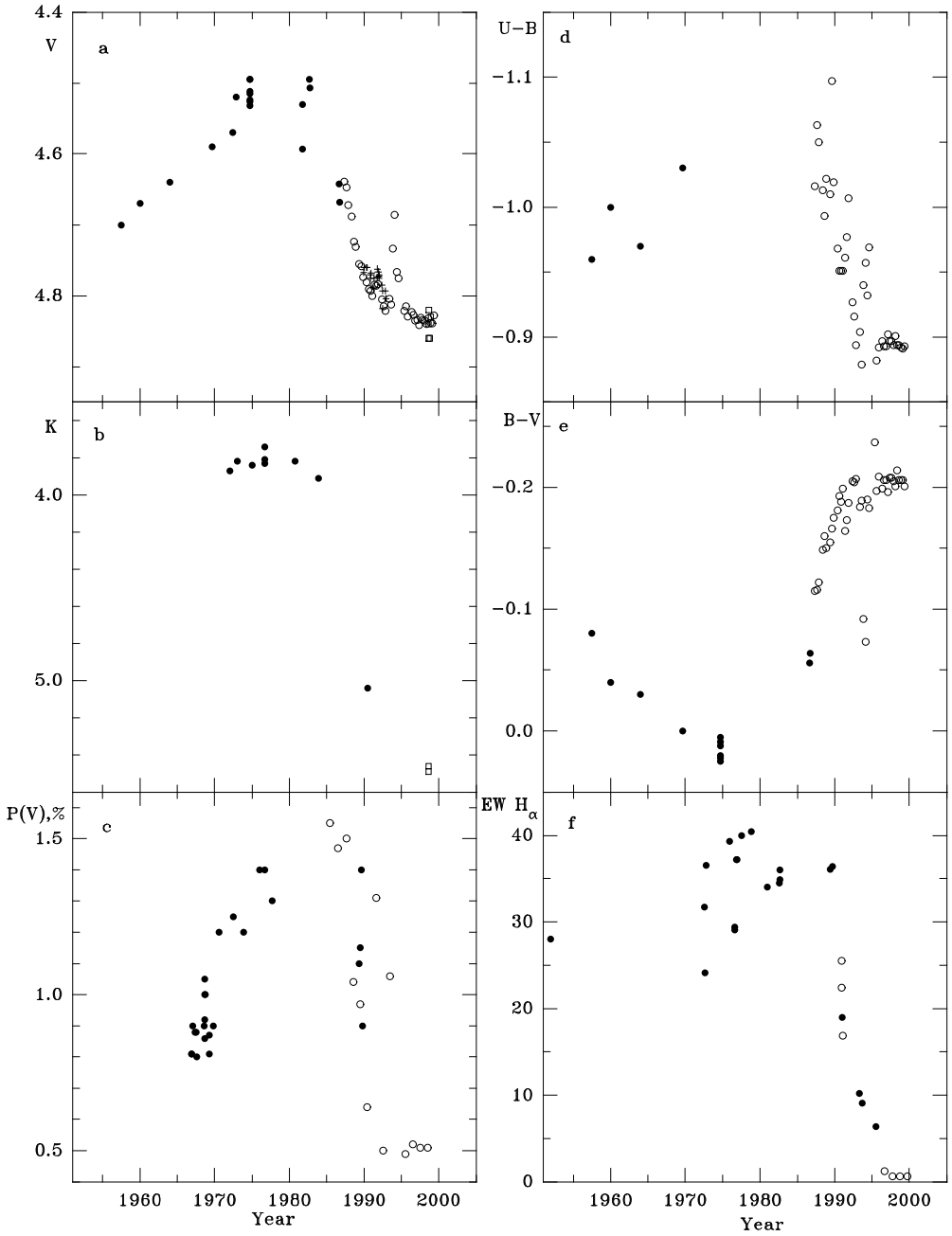

Fig. 1.— Photometric, spectroscopic, and polarimetric variations of π Aqr in 1952–1999. Data taken from the literature are marked with filled circles; Arizona photometry (averaged over every 1/4 year) and Texas polarimetry (from McDavid 1999) with open circles; Tien-Shan photometry with open squares; and HIPPARCOS data transformed into V magnitudes, using the approximation by Harmanec (1998), with pluses. Equivalent widths of the Hα line are given in Å.

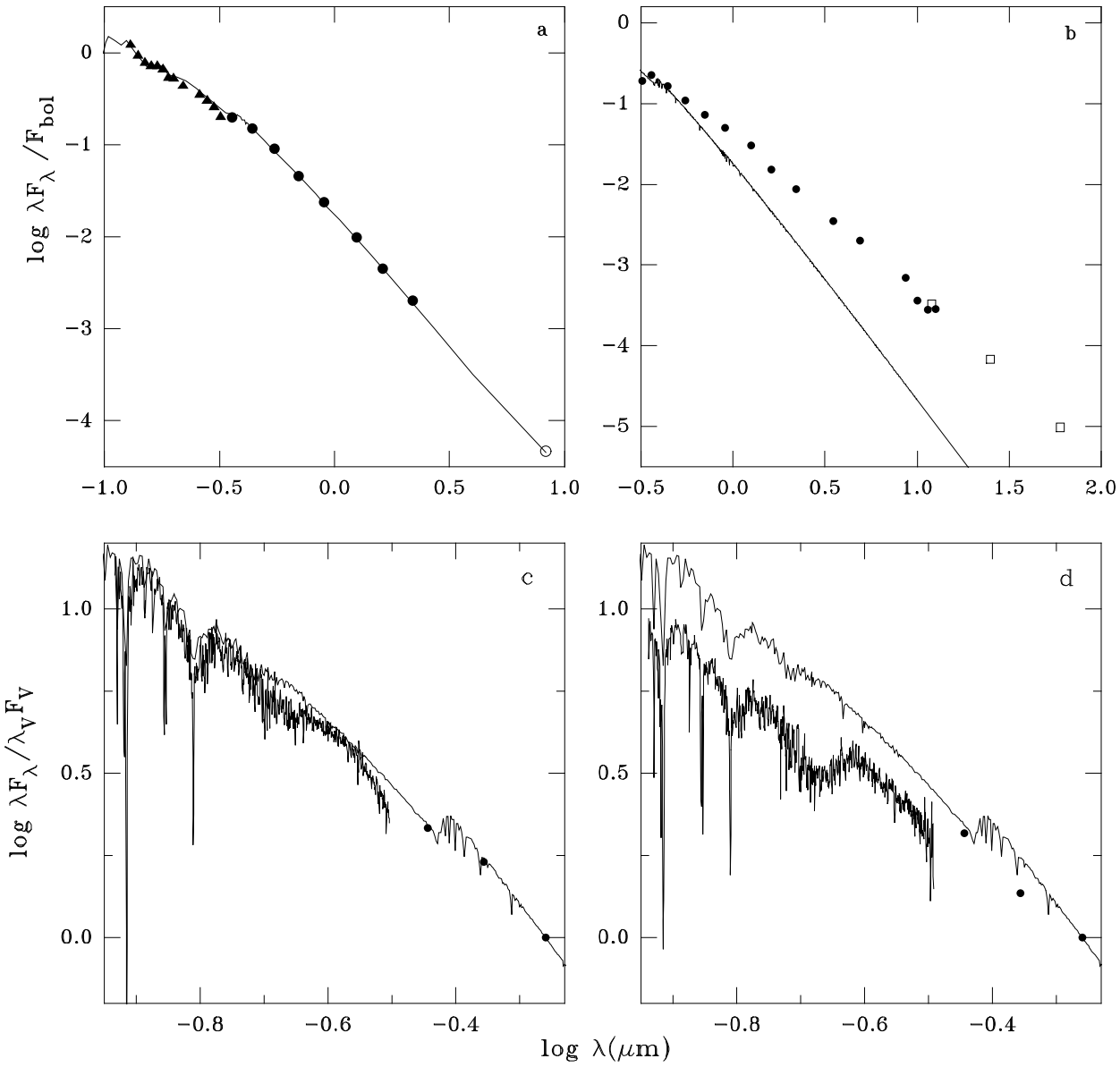

Fig. 2.— Dereddened spectral energy distributions of π Aqr in the active Be (panels b,d) and quasi-normal star (panels a,c) phases. Ground-based photometric data are shown by filled circles, the *MSX* (panel a) and *IRAS* (panel b) data by open circles, and UV continuum fluxes from the IUE spectrum LWP 30769 by triangles. The Kurucz model atmosphere for $T_{\rm eff} = 25,000$ K and $\log g = 4.0$ is shown by solid lines in all panels. The *IUE* spectra of π Aqr supplemented with the UBV photometric data in the corresponding phases are shown in panels c and d.

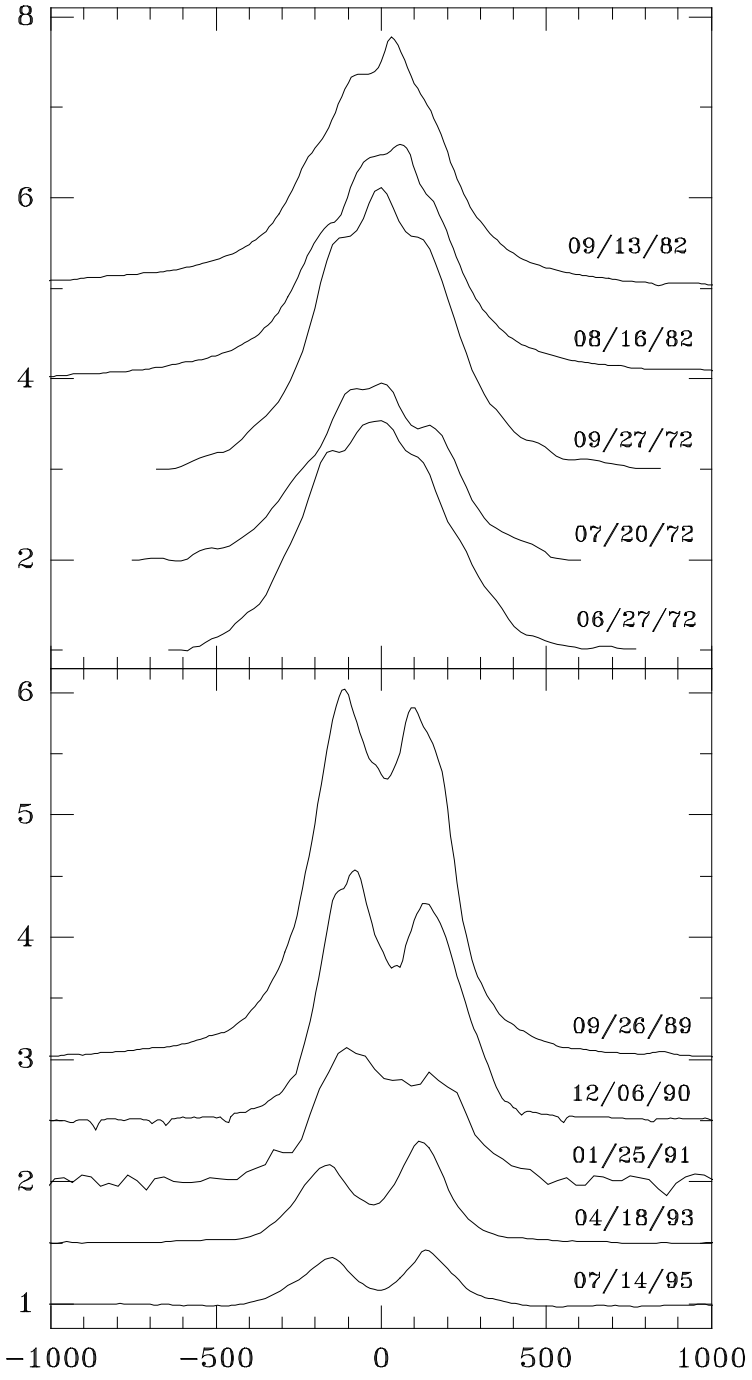

Fig. 3.— Evolution of the Hα profile of π Aqr during the last active Be star phase. The profiles obtained in 1972–1989 are shown in the upper panel (from Gray and Marlborough 1974; Hanuschik et al. 1996), while those obtained in 1989–1995 are shown in the lower panel (from Hanuschik et al. 1996, and this paper). The intensities are normalized to the underlying continuum; the radial velocities are given in km s^{-1}.

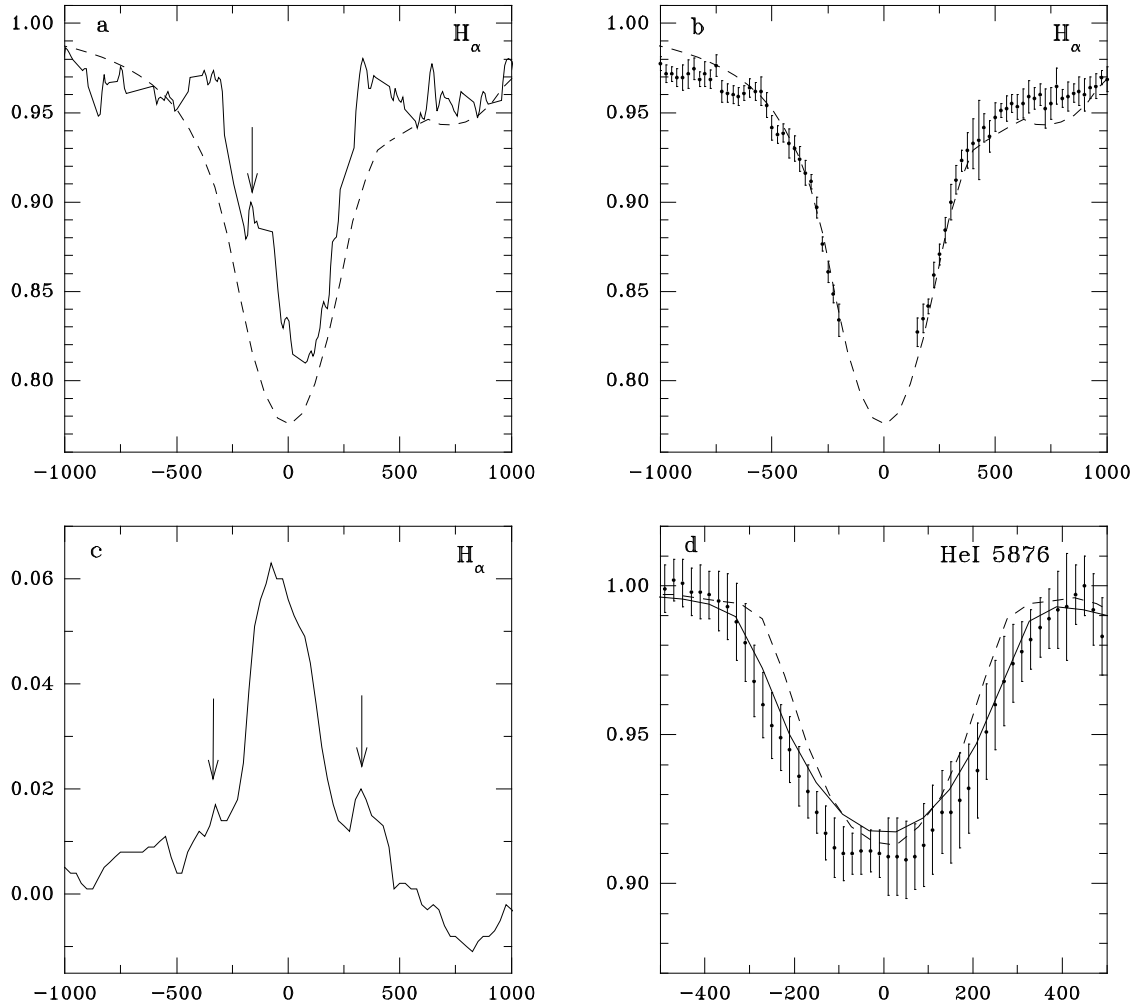

Fig. 4.— Typical line profiles of π Aqr during the quasi-normal star phase. The intensities and radial velocities are in the same units as in Fig. 3. a) The averaged Hα profile observed during two emission events in 1996 and 1998. The arrow marks the location of the traveling emission peak. b) The averaged Hα profile with the region affected by emission extracted. All profiles with the traveling emission peak at velocities $v \geq 75$ km s^{-1} were used to average the blue wing, while those with $v \leq -95$ km s^{-1} were used to average the red wing. The theoretical line profile for $T_{\rm eff} = 25,000$ K, log $g = 4.0$, and v sin $i = 250$ km s^{-1} is shown in both panels by a dashed line. c) The average profile (with the photospheric contribution subtracted) calculated from 63 observations obtained in 1996–1999 is shown in the lower panel. The arrows mark the double-peaked structure arising in the visible star's disk. d) The averaged He I 5876Å line profile during the quasi-normal star phase. The observed averaged profile is shown by filled circles along with the errors. The theoretical profile for $T_{\rm eff} = 25,000$ K, log $g = 4.0$, and v sin $i = 250$ km s^{-1} is shown by a dashed line, while that for $T_{\rm eff} = 20,000$ K, log $g = 4.0$, and v sin $i = 300$ km s^{-1} is shown by a solid line.

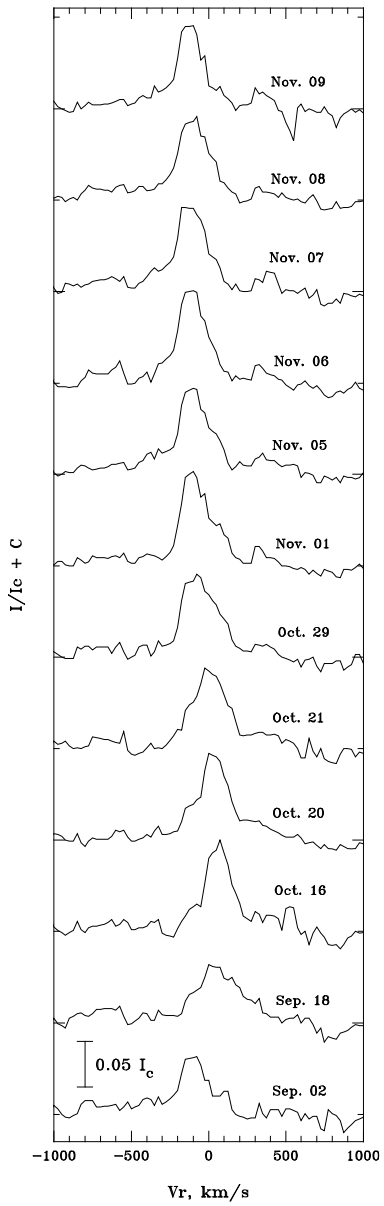

Fig. 5.— Residual Hα line profiles obtained in 1999. The theoretical profile for $T_{\rm eff} = 25,000$ K, $\log\ g = 4.0$, and $v\ \sin\ i = 250$ km s^{-1} was subtracted from each observed profile. Individual profiles are shifted by 0.1 F_c with respect to each other. Intensity and velocity are in the same units as in Fig. 3.

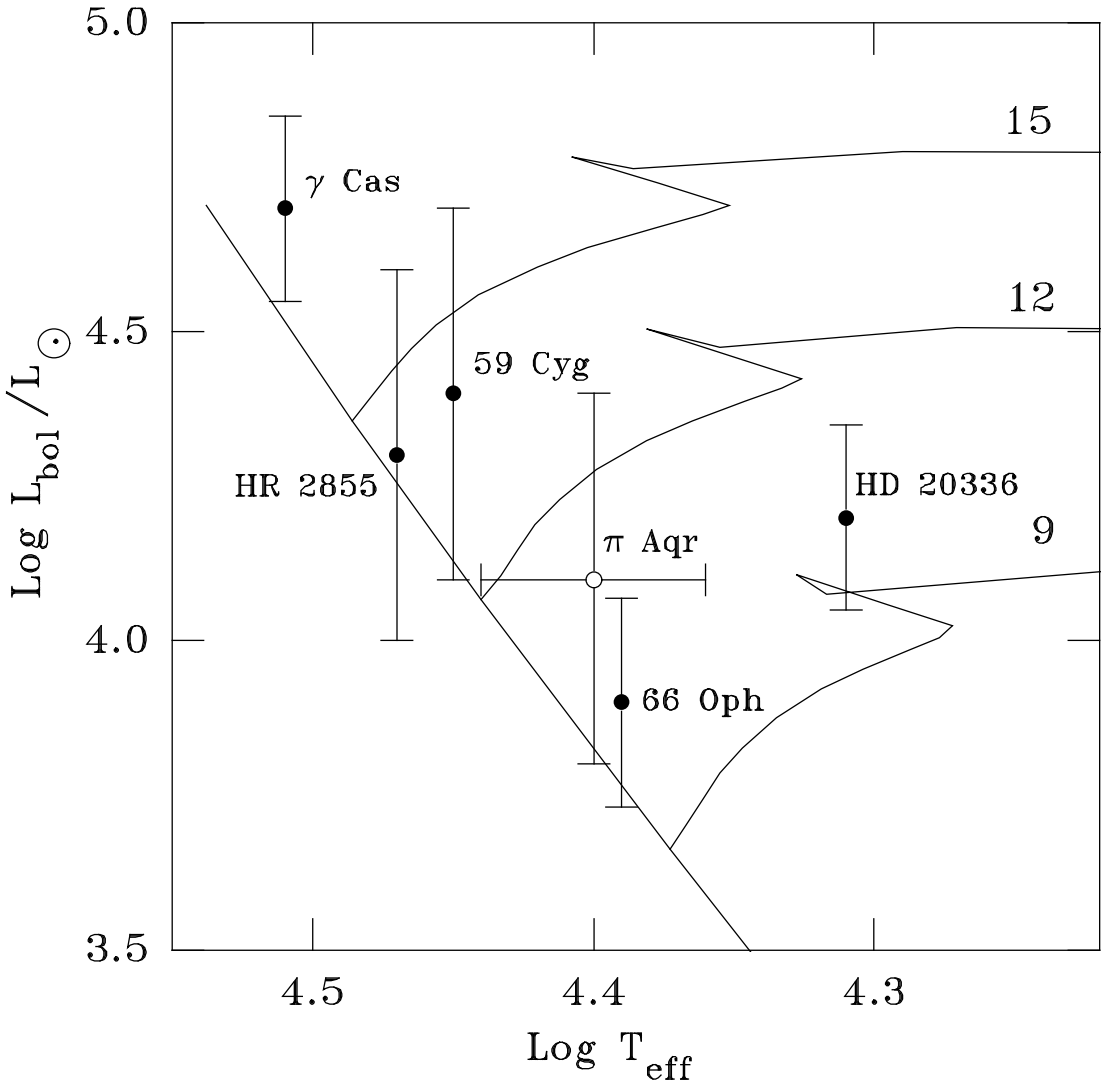

Fig. 6.— Location of π Aqr in the Hertzsprung-Russell diagram. The open circle with error bars marks our results. Evolutionary tracks for 9, 12 and 15 $M_{\odot}$ from Shaerer et al. (1993) are shown by solid lines. The positions of several other Be stars (from Zorec and Briot 1991) with similar spectral types are given for comparison.

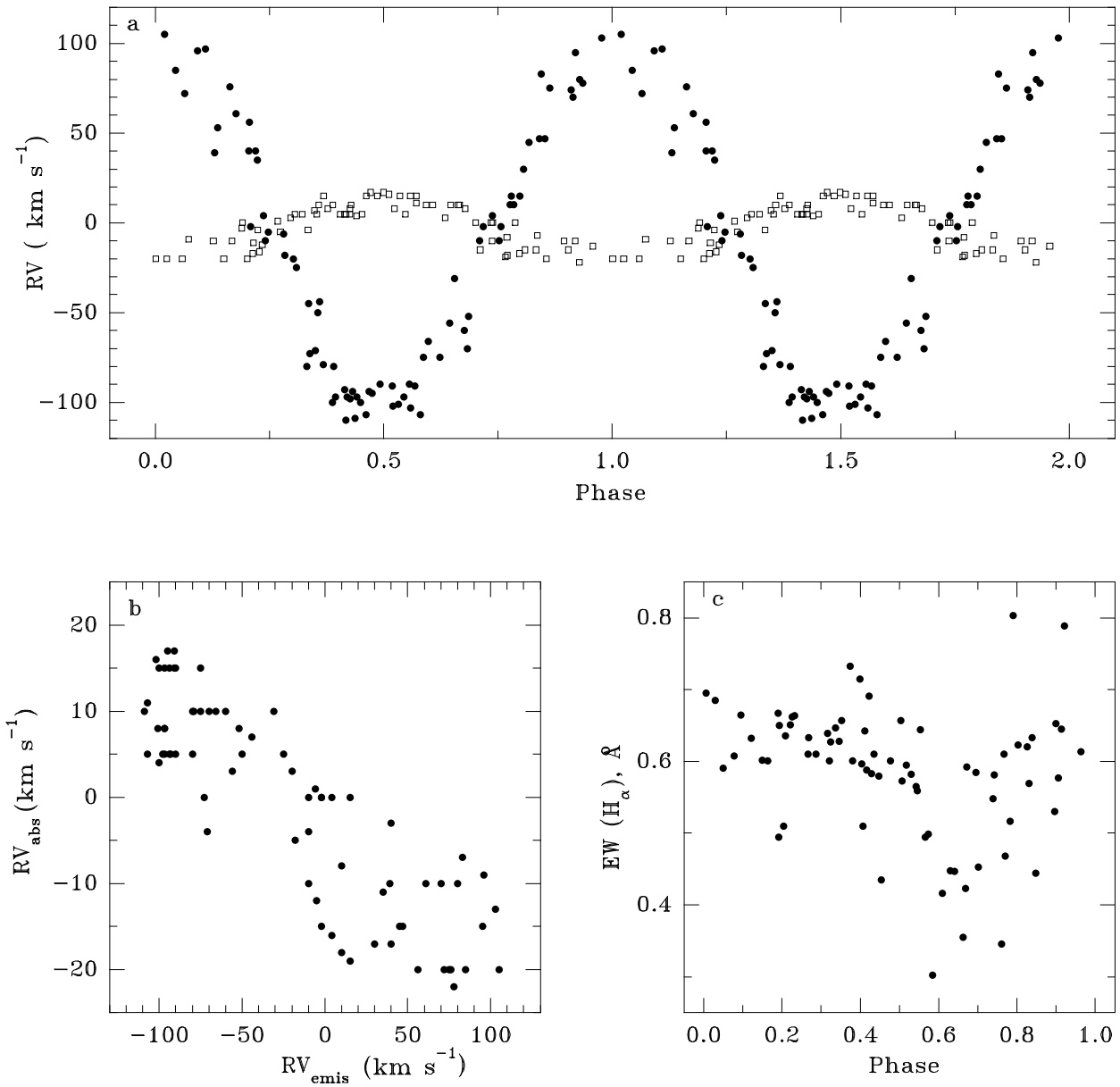

Fig. 7.— The Hα line radial velocity and equivalent width phase curve. a) The RVs of the traveling emission component are shown by filled circles, while the RVs of the absorption component are shown by open squares. The mean error of the measurements is 5 km s^{-1}. b) The RVs of the Hα components plotted against each other. c) The equivalent width of the traveling emission component.

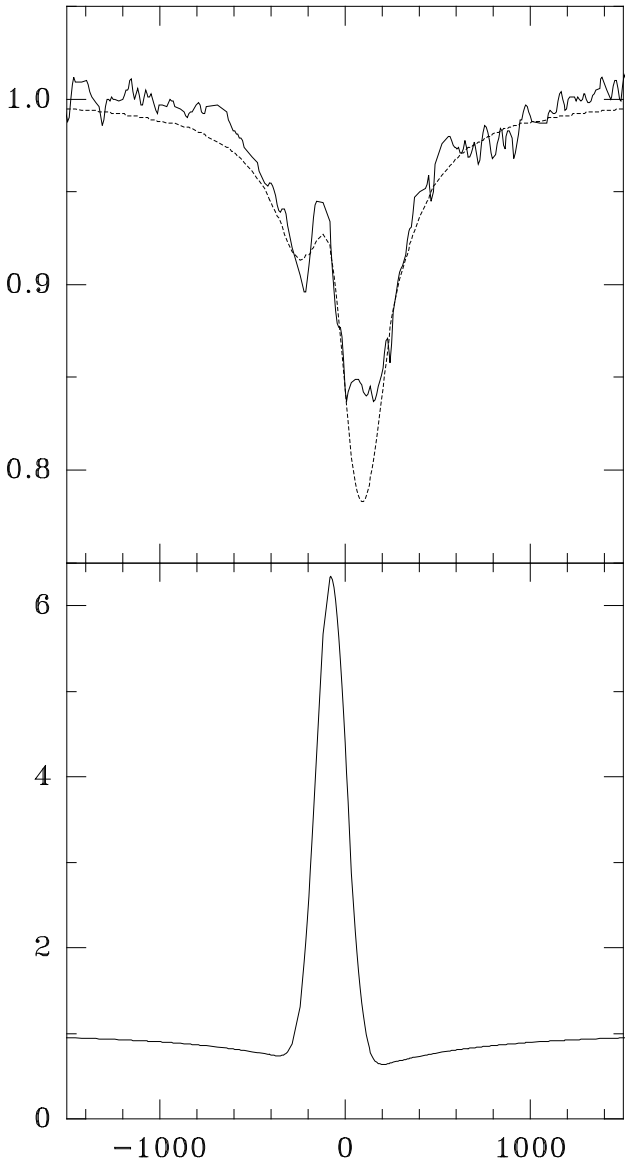

Fig. 8.— The Hα line profile obtained on 1996 November 4 and its theoretical fit. The observed profile (solid line) and the composite calculated profile (dashed line) are shown in the upper panel. The composite profile consists of two Kurucz (1994) theoretical profiles, ($T_{\rm eff} = 25,000$ K, log $g =$ 4.0 and $T_{\rm eff} = 9,000$ K, log $g = 4.0$), and a Gaussian emission. The continuum brightness ratio is 40. Both photospheric profiles are broadened at $v \sin i = 250$ km s^{-1}. The lower panel represents the appearance of the Gaussian emission in the secondary spectrum. Both composite profiles are normalized to the underlying continuum. The velocity scale is in km s^{-1}.

Table 1: Summary of the spectroscopic observations of π Aqr

JD 2400000+ (1)	EW Å (2)	V_{em} km s^{-1} (3)	I_{em} (4)	V_{abs} km s^{-1} (5)	JD 2400000+ (1)	EW Å (2)	V_{em} km s^{-1} (3)	I_{em} (4)	V_{abs} km s^{-1} (5)
50351.73	0.65	70	0.13	−10	51480.59	0.63	−80	0.10	5
50357.08	0.60	103	0.12	−13	51483.57	0.64	−79	0.10	10
50360.67	0.66	105	0.12	−20	51487.54	0.69	−93	0.10	5
50362.66	0.68	85	0.12	−20	51488.55	0.62	−98	0.10	5
50366.70	0.62	96	0.11	−9	51489.51	0.65	−109	0.10	10
50391.56	0.68	−100	0.12	15	51490.52	0.61	−100	0.09	4
50402.53	0.64	−91	0.09	17	51491.54	0.57	−107	0.09	5
50590.86	0.54	−2	0.09	0	51496.48	0.55	−102	0.08	16
50628.87	0.58	−2	0.11	0	51497.50	0.56	−101	0.09	8
50639.83	0.57	−73	0.09	0	51498.51	0.54	−97	0.09	15
50640.84	0.65	−71	0.11	−4	51499.51	0.51	−90	0.07	5
50660.79	0.46	−75	0.07	15	51500.50	0.57	−91	0.08	15
50663.82	0.40	−75	0.08	10	51501.53	0.45	−107	0.08	11
50668.83	0.42	−70	0.06	10	51510.46	0.55	−52	0.07	8
50674.74	0.54	−10	0.06	−10	51512.45	0.55	−10	0.07	0
50688.78	0.56	95	0.08	−15	51520.51	0.78	30	0.08	−17
50704.71	0.63	97	0.08	–	51521.52	0.62	45	0.07	−15
50712.73	0.62	40	0.08	−3	51523.51	0.60	47	0.08	−15
50715.68	0.60	−10	0.07	−4	51524.50	0.60	47	0.08	−10
50728.66	0.60	−97	0.10	8	51531.51	0.77	78	0.11	−22
50730.61	0.60	−110	0.08	–	51777.71	0.44	75	0.06	−20
50732.65	0.56	−97	0.09	8	51781.71	0.53	74	0.08	–
50742.59	0.54	−103	0.08	–	51794.72	0.59	72	0.09	−20
50761.57	0.44	10	0.05	−8	51800.69	0.63	53	0.10	–
51004.83	0.34	−60	0.07	10	51806.64	0.49	56	0.09	−20
51045.79	0.57	76	0.09	−20	51807.69	0.51	40	0.08	−17
51052.84	0.64	−5	0.09	−12	51814.68	0.61	−20	0.09	3
51055.72	0.60	−6	0.08	1	51824.62	0.51	−97	0.09	5
51097.63	0.59	15	0.07	−19	51825.56	0.59	−94	0.14	5
51146.50	0.63	−44	0.10	7	51828.64	0.44	−94	0.10	15
51396.79	0.61	−45	0.09	–	51830.64	0.60	−90	0.10	15
51422.74	0.43	−56	0.07	3	51839.61	0.30	−66	0.08	10
51423.70	0.43	−31	0.06	10	51849.59	0.45	−2	0.10	−15
51435.71	0.48	15	0.07	0	51854.56	0.35	10	0.06	−18
51439.70	0.53	83	0.06	−7	52103.81	0.51	4	0.08	0
51446.66	0.61	80	0.11	−10	52136.72	0.68	39	0.10	−10
51467.64	0.57	61	0.10	−10	52151.73	0.62	−25	0.10	5
51471.56	0.63	35	0.10	−11	52155.77	0.68	−50	0.09	5
51472.64	0.62	4	0.09	−16	52158.65	0.60	−80	0.10	10
51476.57	0.61	−18	0.08	−5	52165.67	0.66	−95	0.10	17

Note. — The heliocentric Julian date for the observation is listed in column 1; EW (column 2) is the equivalent width of the emission component of the Hα profile (a theoretical profile for $T_{\rm eff} = 24,000$ K, log $g = 4.0$, $v\,sin\,i =$ 250 km s^{-1} is subtracted); $V_{\rm em}$ (column 3) is the heliocentric velocity of the traveling emission peak and $I_{\rm em}$ (column 4) is its the residual intensity in continuum units after subtraction of a theoretical photospheric profile; $V_{\rm abs}$ (column 5) is the heliocentric velocity of the absorption part of the Hα profile.

Table 2: Parameters of the RV curves for the Hα line components

Component	γ km s^{-1}	K km s^{-1}	P days	t_0 JD2450000+	r.m.s km s^{-1}
emission	-1.6 ± 0.1	101.4 ± 0.2	84.135 ± 0.004	274.84 ± 0.04	14.4
absorption	-4.9 ± 0.1	16.7 ± 0.2	84.07 ± 0.02	276.5 ± 13.2	6.0